Robust Output-Feedback Control of Fluid Resuscitation with Absolute Stability Guarantee Against Uncertain Physiology and Therapeutic Responsiveness

Drew X. Hohenhaus¹, Weidi Yin¹, Ali Tivay¹, Rajesh Rajamani², Jin-Oh Hahn¹

- 1: Department of Mechanical Engineering, University of Maryland, College Park, MD 20742, USA
- ²: Department of Mechanical Engineering, University of Minnesota, Minneapolis, MN 55455, USA

Abstract

This paper presents a robust closed-loop control approach to fluid resuscitation in patients with hemorrhagic blood loss. A unique strength of the proposed approach is its robustness against uncertain and time-varying patient physiology and therapeutic effectiveness. First, we adopted an observer-based control architecture that can fulfill set point tracking and disturbance rejection objectives. Second, we determined the control gains to achieve adequate transient response performance using the linear quadratic regulator design. Third, we determined the observer gains as a solution to a set of linear matrix inequalities so that the overall closed-loop fluid resuscitation control system is (i) robust against the variability in patient physiology and (ii) absolutely stable against unknown therapeutic effectiveness. We demonstrated the initial proof-of-concept of the proposed approach by conducting rigorous in silico testing using a large number of physiologically plausible virtual patients, while ascertaining the absolute stability via the circle criterion analysis. The results suggested that the proposed approach to closed-loop control of fluid resuscitation is a promising option to advance automation of fluid resuscitation armed with stability against a large variability in patient physiology and therapeutic effectiveness as well as adequate performance in set point tracking and disturbance rejection.

1. Introduction

Hemorrhagic shock is accountable for approximately 40% of mortality globally (Kauvar et al., 2006). In the battlefield, >85% of mortality is attributed primarily to hemorrhage, 25% of which is preventable if timely and appropriate treatment is provided (Eastridge et al., 2011). Hence, early detection of hemorrhage before its recognition via obvious symptoms and provision of life-saving interventions are very important in improving the mortality and morbidity of hemorrhaging patients.

Fluid resuscitation is a central component of treatment for patients with hemorrhagic shock. But, fluid administration is typically performed with manual patient monitoring and titration. Hence, the quality of fluid resuscitation hinges upon many factors, such as the level of exhaustion, distraction, and inexperience of a clinician in charge of the treatment. Hence, there has been an increasing interest in automating fluid resuscitation (Avital et al., 2022). However, the majority of prior work has not systematically accounted for the inter- and intra-individual variability in pathophysiological characteristics and therapeutic effectiveness (defined as an increase in blood pressure (BP) with respect to an increase in blood volume (BV)) as well as possible disturbances that can occur in the course of fluid resuscitation (e.g. clots breaking and tourniquets slipping). Among others, strict stability and robustness analysis have not been conducted in most of the existing work on closed-loop controlled automation of fluid resuscitation. Such a lack of rigorous control-theoretic analysis may partly be attributed to the complexity of plant dynamics (i.e., a patient receiving resuscitation treatments). In the absence of mathematical models suited to control design, closed-loop control algorithms have been developed using rule-based techniques (Chaisson et al., 2003; Marques et al., 2017; Patel et al., 2022) and expert knowledge (Berard et al., 2022;

Marques et al., 2017) in much of the prior work, whose stability and robustness may not be readily assessed by standard control-theoretic analysis tools.

Efforts to enable closed-loop control of fluid resuscitation based on control theoretic approaches are emerging. A recent work presented the potential of a compartmental model-based adaptive control algorithm in fluid resuscitation (Gholami et al., 2018). Although details were not provided, its stability and robustness characteristics were established with the Lyapunov theory. In our own prior work, we developed a simple adaptive control algorithm for fluid resuscitation with Lyapunov-based stability analysis (Alsalti et al., 2022; Jin et al., 2019). Our results using BV and BP as controlled variables suggested that tracking of a treatment target is feasible with BV or BP alone, but accurate online estimation of parameters in the plant dynamics may require both BV and BP measurements.

This paper presents a robust closed-loop control approach to fluid resuscitation in patients with hemorrhagic blood loss. A unique strength of the proposed approach is its robustness against uncertain and time-varying patient physiology and therapeutic effectiveness. First, we adopted an observer-based control architecture that can fulfill set point tracking and disturbance rejection objectives. Second, we determined the control gains to achieve adequate transient response performance using the linear quadratic regulator (LQR) design. Third, we determined the observer gains as a solution to a set of linear matrix inequalities (LMIs) so that the overall closed-loop fluid resuscitation control system is (i) robust against the variability in patient physiology and (ii) absolutely stable against unknown therapeutic effectiveness. We demonstrated the efficacy of the proposed approach by conducting in silico testing using a large number of physiologically plausible virtual patients, while ascertaining the absolute stability via the circle criterion analysis.

This paper is organized as follows. Section 2 describes the plant dynamics and control-oriented modeling. Section 3 provides the details of control design. Section 4 presents key results, which are discussed in Section 5. Section 6 concludes the paper with possible future work.

2. Plant Dynamics and Control-Oriented Modeling

We employed a simple parameter-varying linear mathematical model of patient physiology during fluid resuscitation developed in our prior work (Alsalti et al., 2022) as the representation of plant dynamics. The mathematical model consists of the dynamics of BV change and a time-varying gain representing therapeutic effectiveness (i.e., the relationship between the change in BV and the corresponding change in BP). The change in BV is caused by fluid administered into and blood lost from the vasculature as well as the fluid exchanged between the vasculature and the tissues:

$$\dot{\Delta v} = J_F - J_H - J_E \tag{1}$$

where J_F is the rate of fluid administration, J_H is the rate of blood loss, J_E is the rate of fluid shift from the vasculature to the tissues, and $\Delta v = v - v_0$ is the change in BV from its initial value v_0 . The rate of fluid shift J_E is dependent on the body's intrinsic compensatory response to changes in BV and is expressed as:

$$J_E = K_E(\Delta v - r_F) \tag{2}$$

where K_E is a gain representing the intensity of fluid shift, and r_F is hypothetical reference change in BV determined by fluid administered and blood lost. Its dynamics is expressed as:

$$\dot{r_F} = \frac{1}{1 + \alpha_F} J_F - \frac{1}{1 + \alpha_H} J_H \tag{3}$$

where α_F is the fraction of fluid administered which remains in the vasculature in the steady state, and α_H is the fraction of blood lost which is restored by fluid shift from the tissues to the vasculature in the steady state. An input-output relationship below can be derived by combining (1)-(3):

$$\ddot{\Delta v} + K_E \dot{\Delta v} = \dot{J_F} - \dot{J_H} + K_E \left(\frac{1}{1 + \alpha_F} J_F - \frac{1}{1 + \alpha_H} J_H \right) \tag{4}$$

Note that the parameters K_E , α_F , and α_H are unknown and subject to inter-individual variability (and possibly, intra-individual variability as well).

The change in BV (i.e., Δv) in (4) is related to the resultant change in BP as follows. BP is given by the product of stroke volume (SV) and arterial elastance (AE):

$$p = v_S E_A \tag{5}$$

Where p is (mean arterial) BP, v_S is stroke volume, and E_A is arterial elastance. Accordingly, the change in BP is expressed as:

$$\Delta p = v_S E_A - v_{s0} E_{A0} = \Delta v_s E_A + \Delta E_A v_{s0} \tag{6}$$

where $\Delta p = p - p_0$, $\Delta v_s = v_s - v_{s0}$, $\Delta E_A = E_A - E_{A0}$, and p_0 , v_{s0} , E_{A0} are the initial values of BP, SV, and AE, respectively. Our prior work illustrated that the changes in SV and AE during blood loss and fluid administration are qualitatively proportional and inversely proportional to the change in BV, respectively (Alsalti et al., 2022):

$$\Delta v_{\rm S} \approx K_{v_{\rm S}} \Delta v, \qquad \Delta E_{\rm A} \approx -K_{E_{\rm A}} \Delta v$$
 (7)

where K_{ν_s} and K_{E_A} are the gains representing the proportional relationships between BV versus SV and AE, respectively. Combining (6) and (7) yields the following relationship between BP and BV:

$$\Delta p = \left(K_{v_S} E_A - K_{E_A} v_{S_0} \right) \Delta v \triangleq K_p \Delta v \tag{8}$$

where K_p is the therapeutic effectiveness pertaining to a patient, specifying how effectively a given increase in BV due to fluid resuscitation can increase BP. It is unknown, because all the terms comprising it are unknown and cannot be measured. In addition, its value is different in different patients depending on her/his physiological profile. Further, it is time-varying due to the variability associated with K_{v_S} , K_{E_A} , and E_A in response to, e.g., fluid administration and blood loss.

Assuming that the change in K_p is slow, (4) can be written in terms of BP as follows:

$$\dot{\Delta p} + K_E \dot{\Delta p} = K_p \left[\dot{J_F} - \dot{J_H} + K_E \left(\frac{1}{1 + \alpha_F} J_F - \frac{1}{1 + \alpha_H} J_H \right) \right] \tag{9}$$

In terms of transfer function, (9) is expressed as:

$$p(s) = \frac{K_p}{s(s + K_E)} \left[\left(s + \frac{K_E}{1 + \alpha_F} \right) J_F(s) - \left(s + \frac{K_E}{1 + \alpha_H} \right) J_H(s) \right] \triangleq G_u(s) J_F(s) - G_d(s) J_H(s)$$
 where $G_u(s) = \frac{K_p}{s(s + K_E)} \left(s + \frac{K_E}{1 + \alpha_F} \right)$ and $G_d(s) = \frac{K_p}{s(s + K_E)} \left(s + \frac{K_E}{1 + \alpha_H} \right)$. (10)

3. Absolutely Stable Output-Feedback Control Design

Our objective is to design a feedback control algorithm which guarantees absolute stability against uncertain patient physiology (in terms of K_E , α_F , and α_H) and therapeutic responsiveness (in terms of K_p) as well as unknown disturbance (J_H due to, e.g., clots breaking and tourniquets slipping). Given that the plant dynamics is linear (although it is uncertain and time-varying), we adopted an observer-based control architecture that can fulfill set point tracking and disturbance rejection objectives. Then, we determined the control gains that can achieve adequate transient response performance using the LQR design. Finally, we determined the observer gains as a solution to a set of LMIs so that the overall closed-loop fluid resuscitation control system is robust against the variability in patient physiology and absolutely stable against unknown therapeutic effectiveness. Details follow.

3.1. Observer-Based Integral Control Architecture

In this paper, we adopted an observer-based integral control architecture (Nise, 2011) (Fig. 1). The rationale is twofold: to achieve (i) perfect tracking of constant BP setpoints and (ii) perfect rejection of slowly varying (e.g., constant) hemorrhage disturbance.

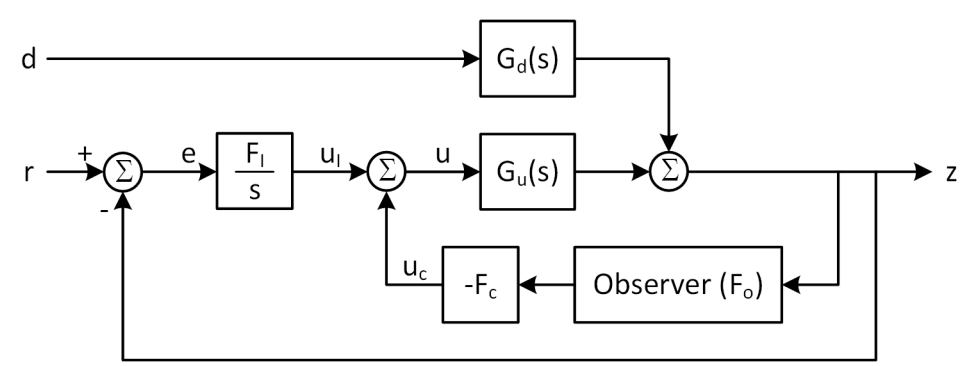


Fig. 1: Observer-based integral control architecture applied to fluid resuscitation.

Denoting $u = J_F$ and $d = J_H$ as input and disturbance, respectively, the transfer function in (10) can be rewritten into the following state space representation:

$$\dot{x} = Ax + B_u u + B_d d, \qquad y = \Delta v = Cx, \qquad z = \Delta p = K_p y \tag{11}$$

where $x = \begin{bmatrix} \Delta v \\ r_F \end{bmatrix}$, $A = \begin{bmatrix} -K_E & K_E \\ 0 & 0 \end{bmatrix}$, $B_u = \begin{bmatrix} \frac{1}{1} \\ \frac{1}{1+\alpha_F} \end{bmatrix}$, $B_d = -\begin{bmatrix} \frac{1}{1} \\ \frac{1}{1+\alpha_H} \end{bmatrix}$, and $C = \begin{bmatrix} 1 & 0 \end{bmatrix}$. We consider the observer-based integral control law:

$$u = u_c + u_I = -F_c \hat{x} + F_I x_N \tag{12}$$

where F_c is sate feedback control gain, \hat{x} is estimated state, F_I is integral control gain, and x_N is error integral expressed as:

$$\dot{x_N} = r - z \tag{13}$$

where r is reference command, i.e., a BP set point to be tracked. The state is estimated using a Luenberger-type observer, where $\overline{K_p}$ is the nominal value of K_p and K_o is observer gain:

$$\dot{\hat{x}} = A\hat{x} + B_u u + F_o \left(z - \overline{K_p} C x \right) \tag{14}$$

The control law (12) can indeed achieve perfect set point tracking and disturbance rejection objectives as shown here. According to Fig. 1, BP output can be expressed as:

$$z(s) = G_u(s)[u_c(s) + u_I(s)] + G_d(s)d(s)$$

$$= G_u(s) \left[-F_c \hat{x}(s) + \frac{K_I}{s} (r(s) - z(s)) \right] + G_d(s)d(s)$$
(15)

where per (14), $\hat{x}(s)$ is expressed as:

$$\hat{x}(s) = \left[sI - \left(A - BF_c - \overline{K_p} F_o C \right) \right]^{-1} F_o z(s) \triangleq G_o(s) z(s) \tag{16}$$

Note that $G_o(s)$ is stable as long as the observer is designed properly. Then, (15) reduces to the closed-form expression relating the output z(s) to the input u(s) and the disturbance d(s):

$$z(s) = \frac{\frac{K_I}{s}G_u(s)}{1 + G_u(s)F_cG_o(s) + \frac{K_I}{s}G_u(s)}u(s) + \frac{G_d(s)}{1 + G_u(s)F_cG_o(s) + \frac{K_I}{s}G_u(s)}d(s)$$
(17)

According to the final value theorem, the steady-state value of z(s) in response to a step $u(s) = \frac{u}{s}$ is given by:

$$\lim_{t \to \infty} z(t) = \lim_{s \to 0} sz(s) = \lim_{s \to 0} \frac{K_I U G_u(s)}{1 + G_u(s) F_c G_o(s) + \frac{K_I}{s} G_u(s)} = U$$
 (18)

Likewise, according to the final value theorem, the steady-state value of z(s) in response to a step $d(s) = \frac{D}{s}$ is given by:

$$\lim_{t \to \infty} z(t) = \lim_{s \to 0} sz(s) = \lim_{s \to 0} \frac{DG_d(s)}{1 + G_u(s)F_cG_o(s) + \frac{K_I}{s}G_u(s)} = 0$$
 (19)

As is obvious from (18) and (19), the observer-based integral control law (12) allows for (i) perfect tracking of constant set points and (ii) perfect rejection of constant disturbances. Hence, the control law (12) fulfills all the desired control objectives.

3.2 Linear Quadratic Regulator-Based State Feedback Integral Control Design

We used the LQR design to determine the state feedback gain F_c and the integral gain F_l . The main motivation was to pre-design the control gains so that the closed-loop fluid resuscitation control system with the observer (to be designed in Section 3.3 so as to make the overall closed-loop fluid resuscitation control system absolutely stable) can achieve desired transient response characteristics if the observer is designed properly (i.e., so that it is fast enough relative to control bandwidth). An additional motivation was to streamline the LMI solution process by reducing the solution space to the two-dimensional observer gain space (see Section 3.3 and Section 5 for details).

To determine the two gains (i.e., F_c and F_I) simultaneously, we concatenated (11) and (13):

$$\begin{bmatrix} \dot{x} \\ \dot{x_N} \end{bmatrix} = \begin{bmatrix} A & 0_{1 \times 2} \\ -K_n C & 0 \end{bmatrix} \begin{bmatrix} x \\ x_N \end{bmatrix} + \begin{bmatrix} B_u \\ 0 \end{bmatrix} u + \begin{bmatrix} B_d \\ 0 \end{bmatrix} d + \begin{bmatrix} 0_{2 \times 1} \\ 1 \end{bmatrix} r \tag{20}$$

Then, we defined the following cost function for LQR-based design of F_c and F_I :

$$J = \int_0^\infty \left(Ru^2 + \begin{bmatrix} x \\ x_N \end{bmatrix}^T Q \begin{bmatrix} x \\ x_N \end{bmatrix} \right) dt \tag{21}$$

where R=1, and $Q=\begin{bmatrix}0&0&0\\0&0&0\\0&0&q\end{bmatrix}$. The rationale is to modulate the relative importance between

control energy (i.e., fluid use) and set point tracking (i.e., error integral x_N) using the parameter q. Note that we used an infinite time interval in calculating our cost function in (21) because it was relevant to the context of our problem. Indeed, there is no a priori knowledge on when the fluid resuscitation treatment will end at the time it is initiated. Hence, it is not unreasonable to consider the cost function over an infinite time interval. In fact, an infinite time interval is quite customary when there is an interest in controlling a system "from-now-on" (Friedland, 1986).

We derived F_c and F_l associated with a range of q values by repetitively assigning a q value in (21) and solving the resulting algebraic Riccati equation corresponding to (21) for a steady-state gain solution using the "lqr" command available in MATLAB Control System Toolbox. Then, we calculated the range of rise time and settling time pertaining to each q (or equivalently, each pair of F_c and F_l) by repetitively simulating a large number of physiologically plausible in silico virtual patients based on a detailed and sophisticated mathematical model with the full state-feedback control law (i.e., $u = -F_c x + F_l x_N$) (see Section 3.4 for details related to virtual patient generation). Finally, we selected two candidate pairs of F_c and F_l associated with conservative (i.e., slow, by emphasizing control energy penalty via a small q) and aggressive (i.e., fast, by emphasizing set

point tracking penalty via a large q) control for subsequent extension to observer-based control design and analysis of closed-loop stability, robustness, and performance. Note that these candidate control gain pairs were used as two instances of the tradeoff between set point tracking vs control energy to demonstrate the influence of control gain on the downstream observer design, especially in terms of (i) LMI-feasible observer gain region and (ii) the ultimate performance of the closed-loop control system.

3.3. Linear Matrix Inequality-Based Absolutely Stable Control Design

Given the control gains F_c and F_l in (12) to achieve the desired transient response characteristics, we designed an observer to be paired with the control law which can guarantee absolute stability against unknown and varying patient physiology and therapeutic effectiveness. Our approach is to (i) express therapeutic effectiveness as an unknown nonlinearity with known sector bounds, (ii) express the absolute stability requirements for the observer-based closed-loop fluid resuscitation control system against this sector nonlinearity as a set of LMIs, (iii) find feasible observer gains by solving this set of LMIs repetitively across diverse physiologically plausible plant dynamics parameters representing patient physiology (K_E , α_F , and α_H), and (iv) select an observer gain that guarantees absolute stability against the sector-bounded therapeutic effectiveness for all sets of plant dynamics parameters tested and achieves adequate transient response characteristics in set point tracking and disturbance rejection. Details follow.

To facilitate the analysis of absolute stability associated with the overall observer-based closed-loop fluid resuscitation control system, we expressed the entire system dynamics in terms of the state x, the state estimation error \tilde{x} , and the error integral x_N , with the output z as an external input to the system dynamics:

$$\begin{bmatrix} \dot{x} \\ \dot{\tilde{x}} \\ \dot{x}_N \end{bmatrix} = \Omega \begin{bmatrix} x \\ \tilde{x} \\ x_N \end{bmatrix} + \Psi d + \begin{bmatrix} 0_{2\times 1} \\ 0_{2\times 1} \\ 1 \end{bmatrix} r - \Sigma z, \qquad y = \Pi \begin{bmatrix} x \\ \tilde{x} \\ x_N \end{bmatrix}, \qquad z = K_p y$$
 (22)

where
$$\Omega = \begin{bmatrix} A - B_u F_c & B_u F_c & B_u F_I \\ F_o \overline{K_p} C & A - F_o \overline{K_p} C & 0_{2\times 1} \\ 0_{1\times 2} & 0_{1\times 2} & 0 \end{bmatrix}$$
, $\Psi = \begin{bmatrix} B_d \\ B_d \\ 0 \end{bmatrix}$, $\Sigma = \begin{bmatrix} 0_{2\times 1} \\ F_o \\ 1 \end{bmatrix}$, and $\Pi = \begin{bmatrix} C & 0_{1\times 2} & 0 \end{bmatrix}$. Note

that (22) separates the unknown therapeutic effectiveness K_p from the rest of the closed-loop dynamics when r=d=0, as shown in Fig. 2.

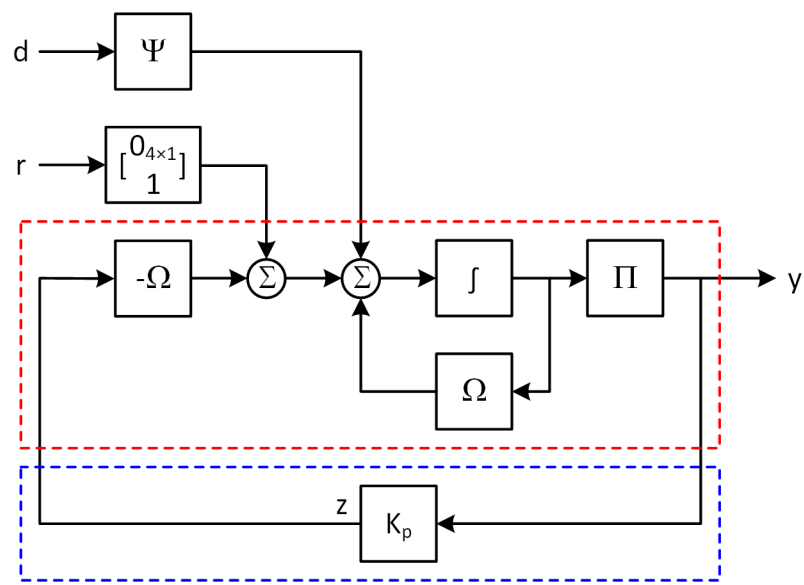


Fig. 2: Closed-loop system dynamics applicable to absolute stability analysis.

We assumed that K_p is completely unknown, and that it can even be time-varying: $K_p = K_p(t)$. However, given that $z = K_p y$, it can be sector-bounded:

$$K_{p,min}y \le z = K_p y \le K_{p,max}y, \qquad 0 \le K_{p,min} \le K_{p,max}$$
(23)

In the context of fluid resuscitation, the sector bound (23) is a physiologically plausible bound because it implies that BP must increase when BV increases. We specified the sector bound by simulating a large number of physiologically plausible in silico virtual patients and calculating the range of therapeutic effectiveness (i.e., $\frac{\Delta p(t)}{\Delta v(t)}$, $\forall t \geq 0$) (see Section 3.4 for details related to virtual patient generation). Now, our task is to find the observer gain F_o which renders the overall observer-based closed-loop fluid resuscitation control system absolutely stable in the sector $[K_{p,min},K_{p,max}]$ (meaning asymptotically stable for all K_p satisfying (23)). Invoking the Lyapunov stability theory, consider the following positive definite (PD) function:

$$V(X,t) = X^T P X \tag{24}$$

where $X = \begin{bmatrix} x \\ \tilde{x} \\ x_N \end{bmatrix}$ and P is a symmetric PD matrix. Taking its time derivative while assuming r = d = 0:

$$\dot{V}(X,t) = X^{T}(\Omega^{T}P + P\Omega)X - 2X^{T}P\Sigma K_{p}y$$
(25)

Our goal is to find the observer gain F_o and the corresponding symmetric PD matrix P such that $\dot{V}(X,t)$ in (25) is negative definite (ND) for all possible K_p within the sector bound (23). Since $y=\Pi X$, negative definiteness of (25) can be expressed as:

$$X^{T} \left[\left(\Omega - K_{p} \Sigma \Pi \right)^{T} P + P \left(\Omega - K_{p} \Sigma \Pi \right) \right] X < -\epsilon X^{T} X$$
 (26)

Since (i) K_p is sector-bounded by $[K_{p,min}, K_{p,max}]$, and (ii) $\dot{V}(X,t)$ is linear in K_p , the left-hand side of the inequality in (26) attains its maximum either at $K_{p,min}$ or at $K_{p,max}$ (Khalil, 2001). Hence, the absolute stability condition is expressed as:

$$\left(\Omega - K_{p,min} \Sigma \Pi\right)^T P + P\left(\Omega - K_{p,min} \Sigma \Pi\right) < -\epsilon I, \qquad \left(\Omega - K_{p,max} \Sigma \Pi\right)^T P + P\left(\Omega - K_{p,max} \Sigma \Pi\right) < -\epsilon I$$
(27)

which are LMIs in P given F_o . Hence, we created a wide range of F_o in a two-dimensional space representing its two gain elements as candidate solutions. For each F_o , we repetitively solved the resulting LMI problems in P across a large number of physiologically plausible plant dynamics equipped with diverse parameter values representing patient physiology (K_E , α_F , and α_H). In addition, we calculated the range of rise time and steady-state error pertaining to each F_o by repetitively simulating the observer-based closed-loop control law (12) pertaining to each F_o across a large number of physiologically plausible in silico virtual patients (see Section 3.4 for details related to virtual patient generation). Finally, we selected an observer gain F_o to be paired with the control gains F_c and F_I selected in Section 3.2 such that (i) the overall closed-loop fluid resuscitation control system is absolutely stable against the uncertain therapeutic effectiveness and (ii) the transient response achieved by the observer-based feedback control law is adequate.

3.4. Circle Criterion Analysis and In Silico Evaluation

We evaluated the observer-based closed-loop fluid resuscitation control system developed in Sections **3.2-3.3** by conducting (i) circle criterion analysis to evaluate its stability characteristics and (ii) virtual in silico simulations with a large number of physiologically plausible "virtual patients" to evaluate its time response performance. Details follow.

First, we ascertained the absolute stability of the observer-based closed-loop fluid resuscitation control system by conducting circle criterion analysis (Khalil, 2001). According to circle criterion, the closed-loop fluid resuscitation control system in Fig. 2 is absolutely stable in the sector $[K_{p,min},K_{p,max}]$ if (i) Ω has no imaginary axis eigenvalues, (ii) (Ω,Σ) is controllable and (Ω,Π) is observable, and (iii) the Nyquist plot of the forward-path transfer function in Fig. 2 (i.e., $\dot{X}=\Omega X+\Sigma u,\ y=\Pi X$) does not enter the disk $D(K_{p,min},K_{p,max})$ (which is a disk centered on the real axis with intercepts at $\left(-\frac{1}{K_{p,min}},0\right)$ and $\left(-\frac{1}{K_{p,max}},0\right)$) nor encircles the disk (now that it is minimumphase). Due to the presence of an eigenvalue at the origin caused by the integral control, we used the pole shifting technique (Khalil, 2001) to Fig. 2, with which a negative feedback of $K_{p,min}y$ was applied to the forward-path transfer function and the same $K_{p,min}y$ was subtracted from the output of the feedback-path nonlinearity $K_{n}y$:

$$\dot{\bar{X}} = \bar{\Omega}\bar{X} + \Psi d + \begin{bmatrix} 0_{2\times 1} \\ 0_{2\times 1} \\ 1 \end{bmatrix} r - \Sigma \bar{z}, \qquad y = \Pi \bar{X}, \qquad \bar{z} = (K_p - K_{p,min})y$$
 (28)

where
$$\overline{\Omega} = \Omega - K_{p,min} \Sigma \Pi = \begin{bmatrix} A - B_u F_c & B_u F_c & B_u F_I \\ F_o \big(\overline{K_p} - K_{p,min} \big) \mathcal{C} & A - F_o \overline{K_p} \mathcal{C} & 0_{2 \times 1} \\ -K_{p,min} \mathcal{C} & 0_{1 \times 2} & 0 \end{bmatrix}$$
. In the course of analysis, we

confirmed that all the conditions for absolute stability were satisfied across all the virtual patients

employed in the evaluation. Then, we examined the Nyquist plots associated with all the virtual patients. Note that the disk has an infinite diameter after the pole shifting, with which (iii) above becomes the Nyquist plot of the forward-path transfer function lying in the right side of the vertical line passing through $\left(-\frac{1}{K_{p,max}-K_{p,min}},0\right)$.

Second, we examined the time response performance of the observer-based closed-loop fluid resuscitation control system by conducting a large number of realistic in silico simulations using physiologically plausible virtual patients. To generate virtual patients, we used a validated highfidelity mathematical model that can replicate physiological responses to hemorrhage and fluid administration (Tivay et al., 2022; Yin et al., 2022) and a novel collective inference-enabled virtual patient generation method (Tivay et al., 2022). The mathematical model is much more detailed and sophisticated than the time-varying linear plant dynamics in (9)-(10) and includes arterial and venous BV dynamics with interstitial fluid exchange as well as autonomic control of cardiac and vascular functions. We created a virtual patient generator by applying the collective inference method to the mathematical model in conjunction with in vivo experimental data collected from a large number of animals used in our prior work (Tivay et al., 2022). The virtual patient generator is in the form of a multivariate probability density function characterizing the parameter values in the mathematical model. Then, we generated a total of 100 random samples (each of which is a vector of numerical values for the parameters in the mathematical model) from the virtual patient generator. We used these virtual patients in calculating (i) the range of rise time and settling time with respect to the LQR design parameter q in Section 3.2, (ii) the sector bound of K_n in Section 3.3, and (iii) the range of rise time and steady-state error associated with the closed-loop control system with respect to the observer gain F_0 in Section 3.3.

In particular, with regard to (iii) above, we evaluated the performance of the observer-based absolutely stable control approach to fluid resuscitation by simulating it in a fluid resuscitation scenario. Each virtual patient was subject to hemorrhage of 0.5-2.5 L in BV which lowered BP in the virtual patients to 25+/-10 mmHg level, and then received fluid administration by the control law (12) to restore BP up to 85 mmHg. Then, 40 min after fluid resuscitation started, each virtual patient was subject to a secondary hemorrhage of 0.5 L in BV for 10 min (to simulate disturbances such as clots breaking and tourniquets slipping). We used the BP response during the initial 40 min to evaluate the set point tracking performance. We used the BP response after the onset of secondary hemorrhage (i.e., 40 min onward) to evaluate the disturbance rejection performance. To make the in silico simulation more realistic, we contaminated simulated BP by a measurement noise in the form of a Gaussian random noise of 2 mmHg in magnitude. Then, we calculated rise time, 2% settling time, and steady-state error (defined as the average of the error between the BP set point (85 mmHg) and the closed-loop controlled BP response within the time window from 2% settling time to the onset of secondary hemorrhage (i.e., 40 min)) associated with the BP response pertaining to each virtual patient and summarized them across all the virtual patients as set point tracking metrics. In addition, we calculated percent overshoot, 5% setting time, and steady-state error (defined as the average of the error between the BP set point (85 mmHg) and the closed-loop controlled BP response within the time window from 5% settling time to the end of simulation (80 min)) associated with the BP response pertaining to each virtual patient and summarized them across all the virtual patients as disturbance rejection metrics.

4. Results

Fig. 3 shows the relationship between the range of rise time and settling time pertaining to the BP response in 100 virtual patients under full-state feedback control vs the LQR design parameter q. Fig. 4 shows the Nyquist plots of the forward-path transfer functions (28) in Fig. 2 associated with 100 plausible plant dynamics relative to the circle criterion condition. Fig. 5 shows (i) absolute stability characteristics, (ii) observer bandwidth relative to control bandwidth, (iii) rise time, and (iv) steady-state error. Each point in the absolute stability subplot shows the percentage of virtual patients who are absolutely stable with the observer gain F_o defined by the X and Y coordinates of the point. The performance metrics are the average performance across all the virtual patients. Fig. 6 and Fig. 7 show representative in silico simulation results of fluid resuscitation based on the proposed control approach in BP set point tracking (Fig. 6) and hemorrhage disturbance rejection (Fig. 7) scenarios. Table 1 summarizes the time and steady-state response performance of conservative and aggressive observer-based control designs pertaining to set point tracking and disturbance rejection.

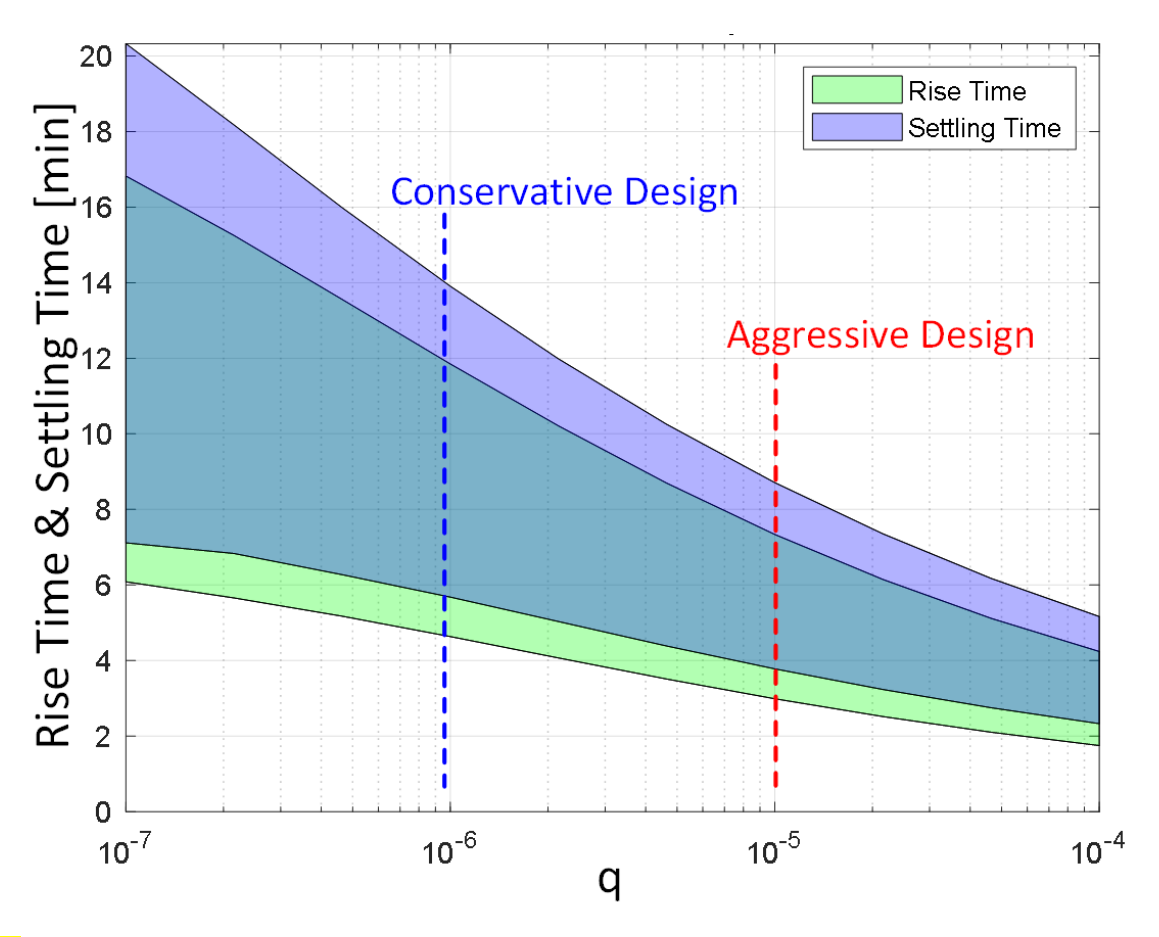


Fig. 3: Relationship between the range of rise time and settling time pertaining to the BP response in 100 virtual patients under full-state feedback control vs the LQR design parameter q. The bounds indicate +/-2 standard deviations across all 100 virtual patients.

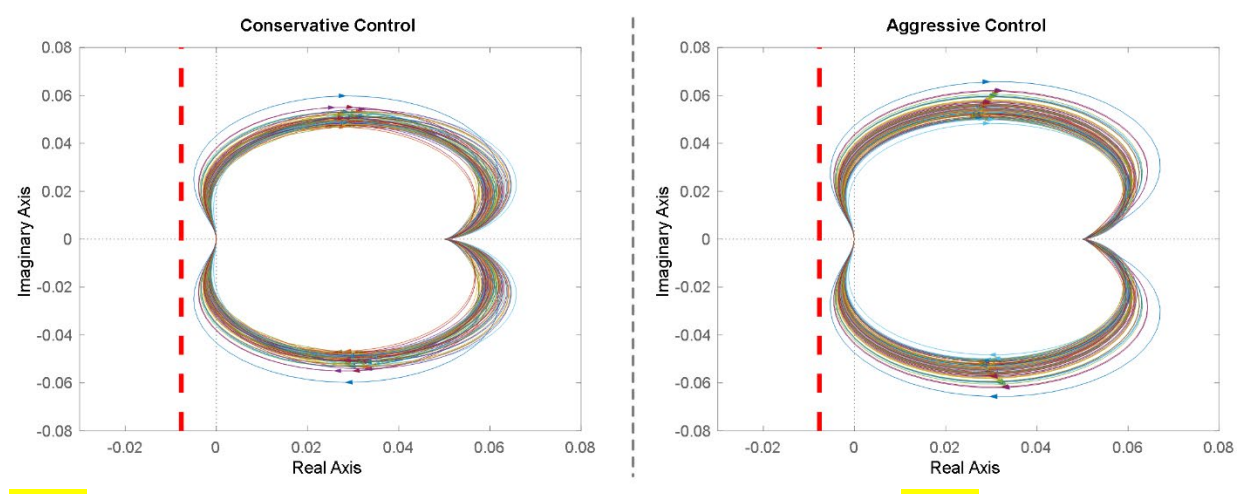


Fig. 4: Nyquist plots of the forward-path transfer functions (28) in Fig. 2 associated with 100 plausible plant dynamics relative to the circle criterion condition. The closed-loop fluid resuscitation control system is absolutely stable since all 100 Nyquist plots are to the right-hand side of the red vertical line.

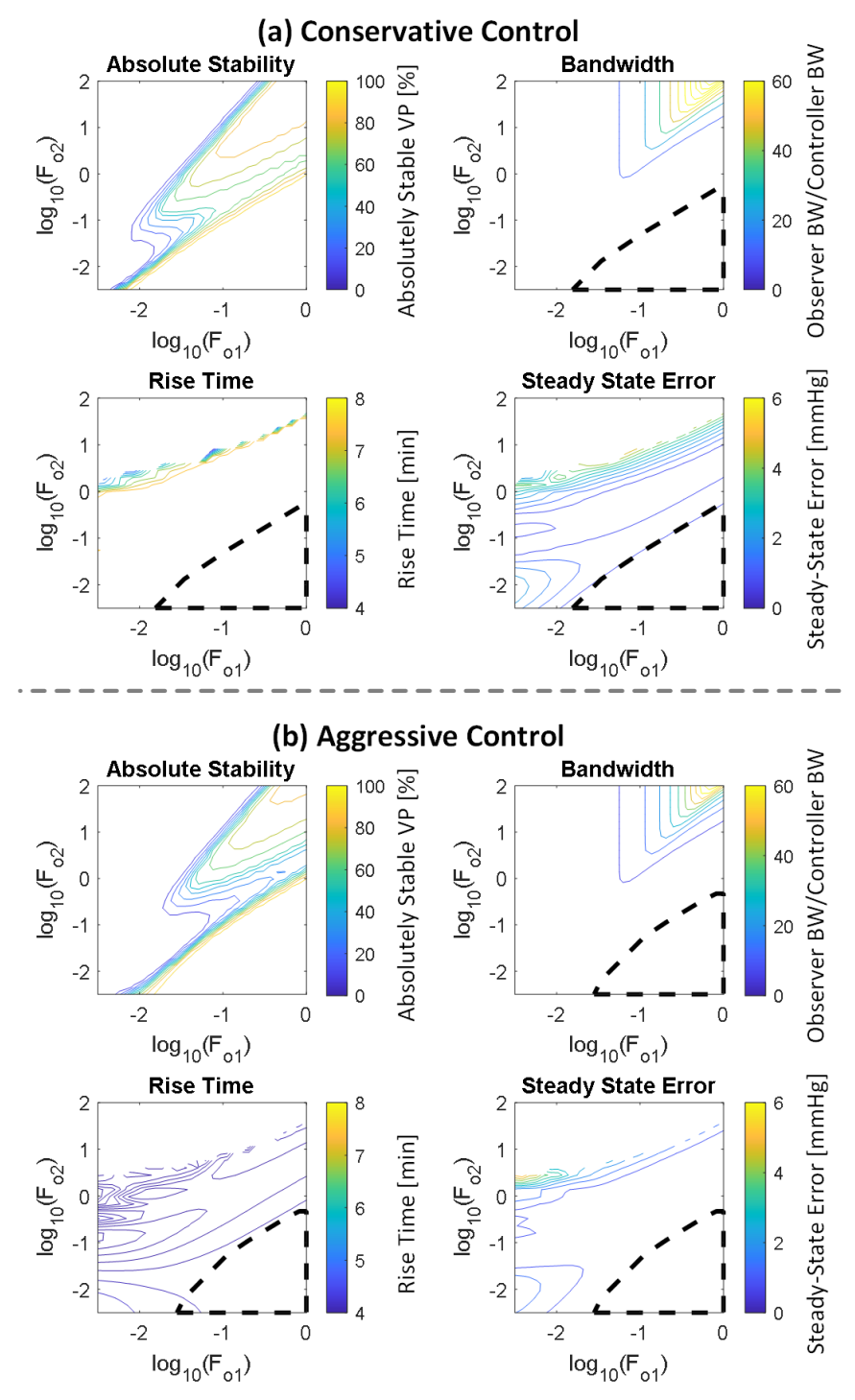


Fig. 5: Absolute stability characteristics (upper left), observer bandwidth relative to control bandwidth (upper right), rise time (lower left), and steady-state error (lower right), all with respect to the observer gain F_o . Each point in the absolute stability subplot shows the percentage of virtual patients who are absolutely stable with the observer gain F_o defined by the X and Y coordinates of the point. The performance metrics are the average performance across all the virtual patients. (a) Conservative control design. (b) Aggressive control design.

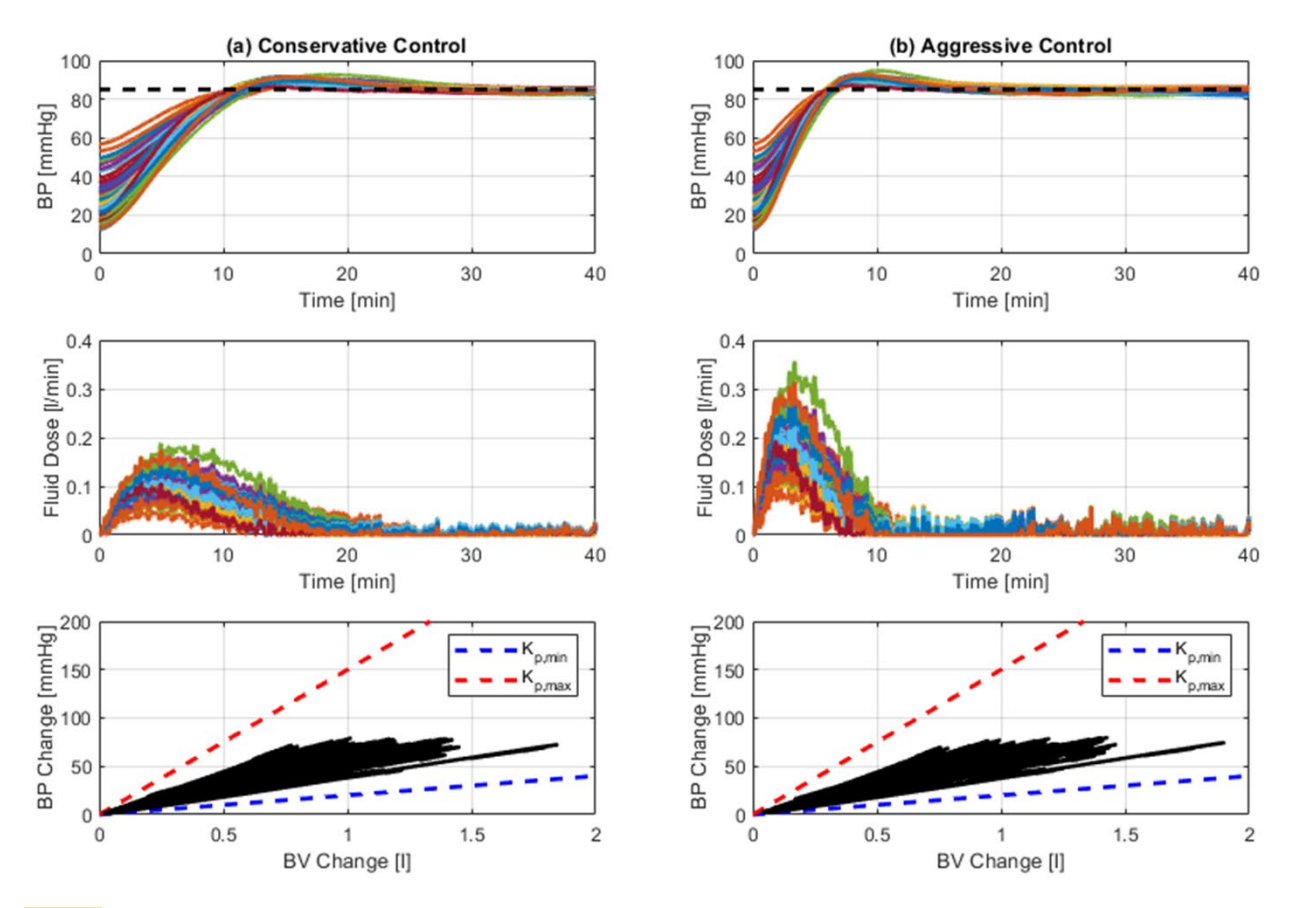


Fig. 6: Representative in silico simulation results of fluid resuscitation based on the proposed control approach in BP set point tracking.

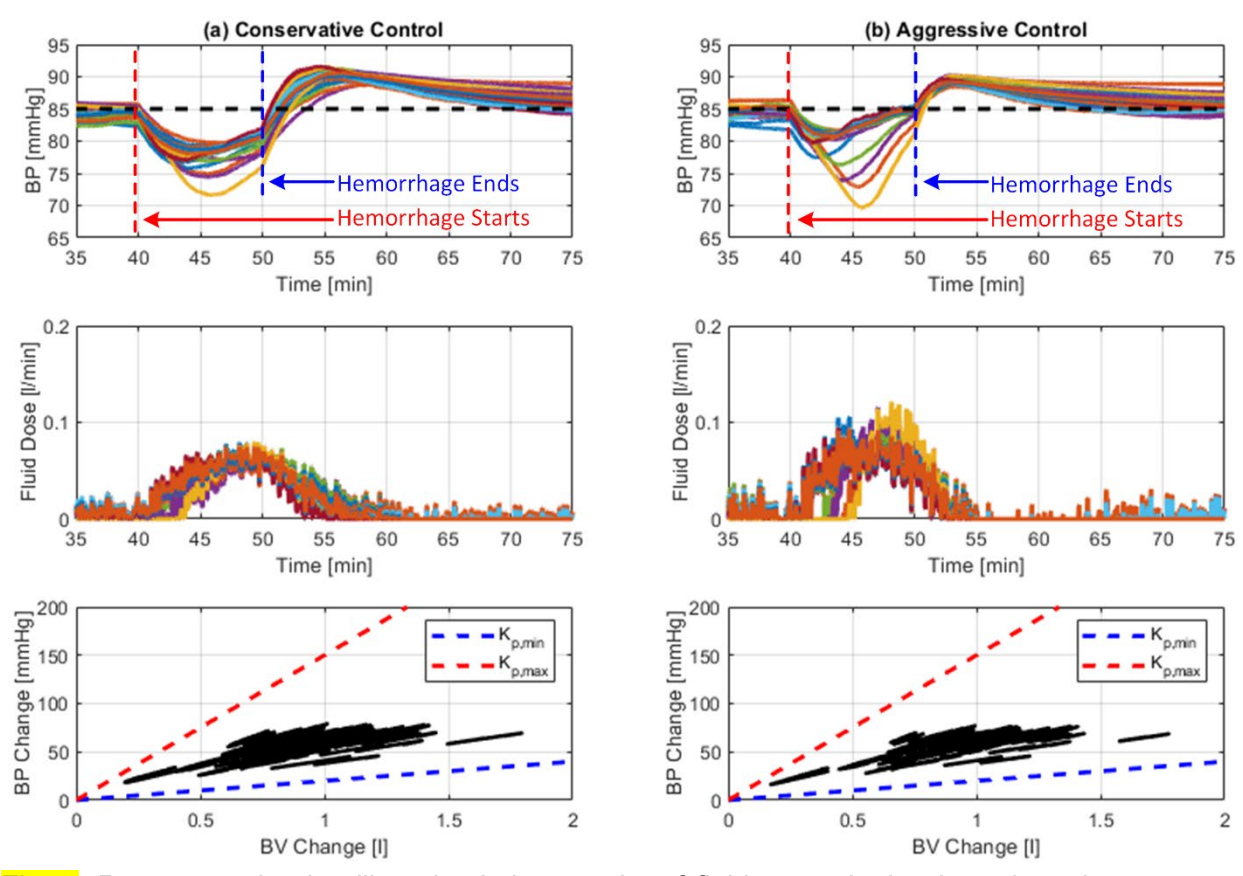


Fig. 7: Representative in silico simulation results of fluid resuscitation based on the proposed control approach in hemorrhage disturbance rejection.

Table 1: Time and steady-state response performance of conservative and aggressive observer-based control designs (median (IQR)).

(a) Set point tracking

<u>\ </u>			
	Rise Time [min]	Settling Time [min]	Steady-State Error [mmHg]
Conservative Control	7.6 (7.4-7.9)	19.9 (17.7-23.2)	0.8 (0.7-0.9)
Aggressive Control	4.1 (4.0-4.2)	12.4 (11.5-14.4)	0.5 (0.4-0.6)

(b) Disturbance rejection

	Overshoot [%]	Settling Time [min]	Steady-State Error [mmHg]
Conservative Control	6.6 (6.2-7.0)	19.1 (9.6-20.4)	2.4 (2.0-2.7)
Aggressive Control	5.0 (4.9-5.2)	2.9 (0.0-3.5)	1.7 (1.5-2.0)

5. Discussion

Fluid resuscitation is a critical component of hemorrhage treatment, but it is heavily dependent on manual administration and re-administration of fluid by human clinicians. Hence, automation of fluid resuscitation can make a leap in hemorrhage treatment in terms of relieving clinician burden while maintaining therapeutic quality and efficacy. However, the vast majority of existing effort to enable closed-loop controlled automation of fluid resuscitation is empiric and ad-hoc with a lack of rigorous control-theoretic analysis to establish stability, robustness, and performance of closed-

loop control system against inter-/intra-individual variability in patient physiology and therapeutic responsiveness. In this paper, we presented an absolutely stable observer-based integral control approach to fluid resuscitation.

5.1. Absolutely Stable Observer-Based Control Design via LQR and LMI

We adopted a 3-step design procedure to realize the proposed approach. First, we designed the control architecture relevant to achieve set point tracking and disturbance rejection objectives. Second, we designed the state-feedback integral control gain using the LQR method. Third, we designed the observer gain using the LMI method. In the design of absolutely stable closed-loop control law, we embeded the unknown therapeutic effectiveness as a sector-bounded nonlinearity in the LMIs, while we addressed the effect of physiological variability by repetitively solving the LMIs with respect to a large number of plausible plant dynamics. In this context, the proposed control design approach provides a probabilistic robustness against variability in both therapeutic effectiveness and patient physiology. The 3-step control design procedure has novel advantages: (i) it automatically embeds set point tracking and disturbance rejection capabilities in the control system architecture; and (ii) it decouples performance and stability/robustness design from each other by specifying the desired performance via control design while enforcing absolute stability via observer design, and then integrating them to achieve desired stability and performance by exploiting the separation principle.

The LQR method allowed us to determine an appropriate state-feedback control gain (both F_c and F_l) with a single design parameter (i.e., q in Q in (21)) (Fig. 3). Both rise time and settling time decreased as q was increased, which is intuitively reasonable. As an illustrative purpose, we used the gains pertaining to $q=10^{-6}$ and $q=10^{-5}$ as conservative and aggressive control gains, respectively.

Circle criterion analysis confirmed that the closed-loop fluid resuscitation control system designed in this paper was absolutely stable against the variability in patient physiology and therapeutic effectiveness. Indeed, the Nyquist plots pertaining to all the 100 virtual patients lied in the right-hand side of the vertical line defined by the sector bound (Fig. 4). Hence, the observer design guided by the LMIs in (27) could provide an appropriate observer gain to be paired with a predesigned control gain to achieve absolute stability via a simple search on the two-dimensional observer gain space.

The results of our observer-based control design approach also provide a few important insights. First, not all the control-observer gain pairs can readily satisfy absolute stability. Indeed, only a specific region in the observer gain space was associated with absolute stability (see the region enclosed by black dashed line in Fig. 5). In addition, the region of absolute stability was influenced by pre-designed control gain (Fig. 5). More specifically, the region of absolute stability became more restrictive as control gain was selected to be more aggressive (Fig. 5). It is also noted that the selection of an observer gain needs to reconcile two competing desirables: guaranteeing absolute stability vs achieving desired performance. Indeed, the region of absolute stability did not in general coincide with the region of high observer bandwidth (relative to control bandwidth) as well as small rise time and steady-state error (Fig. 5). Hence, the observer gains selected and paired with the control gains in this paper were not associated with sufficiently fast observer error dynamics. Regardless, the proposed approach could still result in an absolutely stable observer gain region which could yield adequate closed-loop response characteristics to the extent where

the desired time response performance specified by control pre-design was maintained (Fig. 6 and Fig. 7).

The in silico simulation results based on 100 plausible virtual patients demonstrated satisfactory time and steady-state response performance characteristics of the observer-based closed-loop fluid resuscitation control system (Table 1). In both conservative and aggressive control designs, closed-loop controlled BP responses in all 100 virtual patients could result in the intended time response with reasonably small overshoot and steady-state error in BP set point tracking (Table 1 and Fig. 6). On the other hand, closed-loop controlled BP responses to hemorrhage disturbance exhibited relatively (i) large overshoot in both conservative and aggressive control designs and (ii) slow settling time in conservative control design (Table 1 and Fig. 7). These results may be attributed to two factors. First, the control gain we designed using LQR (Section 3.2) primarily emphasizes BP set point tracking. Hence, transient response characteristics pertaining to hemorrhage disturbance rejection may be suboptimal. Second, our control design did not account for the influence of actuator saturation (i.e., that fluid rate can only be positive) explicitly. As is obvious in Fig. 7, actuator saturation appears to be the main root cause responsible for sluggish disturbance rejection and large settling time. These limitations must be carefully investigated and addressed in a follow-up work.

But all in all, the proposed observer-based absolutely stable integral control approach appeared to have promise in advancing closed-loop controlled automation of fluid resuscitation.

5.2. Limitations

The control design approach presented in this paper has an important limitation that need to be investigated in the follow-up work: (i) control gain and observer gain were designed separately, and (ii) the LMIs (27) were not directly solved to derive the observer gain F_0 . First, pre-design of control gain followed by observer gain design made it possible to separate the achievement of performance and stability/robustness objectives. Regardless, it would be powerful if control and observer gains could be designed simultaneously. Unfortunately, it is easy to recognize that (27) is no longer an LMI if the control gains F_c and F_I are left as unknowns. In addition, it is not clear how to incorporate desired time response performance specifications into the LMIs. Hence, predesigning F_c and F_I had a practical advantage of being able to solve (27) as LMIs using wellestablished LMI solvers while enforcing desired response characteristics. Second, exhaustive search to find the observer gains which can guarantee absolute stability over two-dimensional space was not computationally expensive. Regardless, it would be powerful if the LMIs could be derived by directly solving the inequalities (27) with well-established solvers. It is possible to solve the LMI feasibility problem for (27) to derive P and F_o given F_c and F_I . However, restrictions must be imposed on P if P and F_o are to be uniquely determined, which inevitably put restrictions on the solution space on P and F_o . Considering all these limitations, future investigation to streamline the systematic design of the proposed observer-based control approach may be a meaningful contribution.

Conclusion

In this paper, we demonstrated the validity and promise of an output-feedback absolutely stable control design for automating fluid resuscitation. In contrast to most existing closed-loop control system for fluid resuscitation, we systematically established its stability and robustness against unknown inter- and intra-individual variability in patient physiology and therapeutic effectiveness.

By conducting in silico evaluation with physiologically plausible virtual patients, we demonstrated the promise of our control approach: that it can achieve robust stability and adequate response performance. Future work to streamline the control design procedure, to simultaneously achieve satisfactory set point tracking and disturbance rejection performance, to experimentally evaluate the efficacy of the proposed control approach, and to explore the versatility of the proposed control design approach in other domains of medical automation will be rewarding.

Funding

This work was supported in part by the U.S. National Science Foundation under Grants #1760817 and #1748762.

Conflict of Interest

None declared.

References

- Alsalti, M., Tivay, A., Jin, X., Kramer, G. C., & Hahn, J. O. (2022). Design and in Silico Evaluation of a Closed-Loop Hemorrhage Resuscitation Algorithm with Blood Pressure as Controlled Variable. *Journal of Dynamic Systems, Measurement and Control, Transactions of the ASME*, 144(2). https://doi.org/10.1115/1.4052312
- Avital, G., Snider, E. J., Berard, D., Vega, S. J., Hernandez Torres, S. I., Convertino, V. A., Salinas, J., & Boice, E. N. (2022). Closed-Loop Controlled Fluid Administration Systems: A Comprehensive Scoping Review. *Journal of Personalized Medicine*, 12(7). https://doi.org/10.3390/jpm12071168
- Berard, D., Vega, S. J., Avital, G., & Snider, E. J. (2022). Dual Input Fuzzy Logic Controllers for Closed Loop Hemorrhagic Shock Resuscitation. *Processes*, 10(11). https://doi.org/10.3390/pr10112301
- Chaisson, N. F., Kirschner, R. a, Deyo, D. J., Lopez, J. A., Prough, D. S., & Kramer, G. C. (2003). Near-Infrared Spectroscopy-Guided Closed-Loop Resuscitation of Hemorrhage. *The Journal of Trauma*, *54*(5), S183–S192. https://doi.org/10.1097/01.TA.0000064508.11512.28
- Eastridge, B. J., Hardin, M., Cantrell, J., Oetjen-Gerdes, L., Zubko, T., Mallak, C., Wade, C. E., Simmons, J., Mace, J., Mabry, R., Bolenbaucher, R., & Blackbourne, L. H. (2011). Died of Wounds on the Battlefield: Causation and Implications for Improving Combat Casualty Care. *Journal of Trauma*, *71*(1), S4–S8.
- Friedland, B. (1986). Control System Design: An Introduction to State-Space Methods (S. Rao, Ed.). McGraw Hill.
- Gholami, B., Haddad, W. M., Bailey, J. M., Geist, B., Ueyama, Y., & Muir, W. W. (2018). A Pilot Study Evaluating Adaptive Closed-Loop Fluid Resuscitation during States of Absolute and Relative Hypovolemia in Dogs. *Journal of Veterinary Emergency and Critical Care*, *28*(5), 436–446. https://doi.org/10.1111/vec.12753
- Jin, X., Bighamian, R., & Hahn, J.-O. (2019). Development and in Silico Evaluation of a Model-Based Closed-Loop Fluid Resuscitation Control Algorithm. *IEEE Transactions on Biomedical Engineering*, 66(7), 1905–1914.

- Kauvar, D. S., Lefering, R., & Wade, C. E. (2006). Impact of Hemorrhage on Trauma Outcome: An Overview of Epidemiology, Clinical Presentations, and Therapeutic Considerations. *The Journal of Trauma*, *60*(6), S3-11. https://doi.org/10.1097/01.ta.0000199961.02677.19
- Khalil, H. K. (2001). Nonlinear Systems (3 edition). Pearson.
- Marques, N. R., Ford, B. J., Khan, M. N., Kinsky, M., Deyo, D. J., Mileski, W. J., Ying, H., & Kramer,
 G. C. (2017). Automated Closed-Loop Resuscitation of Multiple Hemorrhages: A
 Comparison between Fuzzy Logic and Decision Table Controllers in a Sheep Model.
 Disaster and Military Medicine, 3, 1. https://doi.org/10.1186/s40696-016-0029-0
- Nise, N. S. (2011). Control Systems Engineering (6th editio). John Wiley & Sons, Inc.
- Patel, N. T. P., Goenaga-Diaz, E. J., Lane, M. R., Austin Johnson, M., Neff, L. P., & Williams, T. K. (2022). Closed-Loop Automated Critical Care as Proof-of-Concept Study for Resuscitation in a Swine Model of Ischemia–Reperfusion Injury. *Intensive Care Medicine Experimental*, 10(1). https://doi.org/10.1186/s40635-022-00459-2
- Tivay, A., Kramer, G. C., & Hahn, J.-O. (2022). Collective Variational Inference for Personalized and Generative Physiological Modeling: A Case Study on Hemorrhage Resuscitation. *IEEE Transactions on Biomedical Engineering*, 69(2), 666–677. https://doi.org/10.1109/TBME.2021.3103141
- Yin, W., Tivay, A., Kramer, G. C., Bighamian, R., & Hahn, J. O. (2022). Conflicting Interactions in Multiple Closed-Loop Controlled Critical Care Treatments: A Hemorrhage Resuscitation-Intravenous Propofol Sedation Case Study. *Biomedical Signal Processing and Control*, 71. https://doi.org/10.1016/j.bspc.2021.103268